Korean J. Chem. Eng., 33(9), 2674-2683 (2016)
DOI: 10.1007/s11814-016-0132-4

pISSN: 0256-1115
eISSN: 1975-7220

Fabrication of novel polyethersulfone based nanofiltration membrane by embedding polyaniline-co-graphene oxide nanoplates

Mojtaba Moochani, Abdolreza Moghadassi†, Sayed Mohsen Hosseini, Ehsan Bagheripour, and Fahime Parvizian

Department of Chemical Engineering, Faculty of Engineering, Arak University, Arak 38156-8-8349, Iran
(*Received 24 January 2016 • accepted 7 May 2016*)

Abstract−Mixed matrix polyethersulfone (PES) based nanofiltration membrane was prepared through phase inversion method by using of polyvinylpyrrolidone (PVP) as pore former and N, N dimethylacetamide (DMAc) as solvent. Polyaniline-co-graphene oxide nanoplates (PANI/GO) were utilized as additive in membrane fabrication. The PANI/GO nanoplates were prepared by polymerization of aniline in the presence of graphene oxide nanoplates. FTIR analysis, scanning electron microscopy (SEM), scanning optical microscopy (SOM), 3D images surface analysis, water contact angle, water content tests, tensile strength tests, porosity tests, salt rejection and flux tests were used in membrane characterization. FT-IR results verified formation of PANI on graphene oxide nanoplates. SOM images showed uniform particles distribution for the mixed matrix membranes. SEM images also showed formation of wide pores for the modified membranes. Water flux showed constant trend nearly by use of PANI/GO in the casting solution. Opposite trend was found for the membrane surface hydrophilicity. Salt rejection was enhanced sharply by utilizing of PANI/GO. The membrane's tensile strength was improved by increase of PANI/GO concentration. The water content was increased initially by use of PANI/GO nanoplates up to 0.05%wt into the casting solution and then decreased. Membrane porosity was also enhanced by using of PANI/GO nanoplates. Modified membrane containing 0.5%wt PANI/GO nanoplates showed more appropriate antifouling characteristic compared to others.

Keywords: Mixed Matrix, Nanofiltration, PANI-co-GO Nanoplates, Physico/Chemical Characterization, Antifouling Property

INTRODUCTION

Nanofiltration (NF) is a membrane technique that it is progressively becoming universal in water treatment [1,2], desalination [3], concentration and purification [4], pharmaceutical [5] and chemical industries [6]. In NF membranes, surface charge and sieving mechanisms are two important parameters that affect the rejection behavior of solutes [7].

Polymers are the main material in the fabrication of most NF membranes. The organic polymer has many advantages such as extensive sources, convenient manufacture, low cost, and easy to achieve industrialization, but it also has disadvantages to overcome, such as bad thermo stability, weak anti-fouling and poor anti-swelling [8-12].

Different polymers such as polysulfone (PS), polyethersulfone (PES), cellulose acetate (CA), polyimide (PI), polyvinylidene fluoride (PVDF), polyamide (PA), polyetherimide (PEI) and poly(phenylene ether ether sulfone) (PEES) [13-25] have been used as basic polymer in membrane fabrication.

Polyethersulfone is an interesting polymer in membrane preparation due to its outstanding mechanical strength, thermal stability and formability. However, low permeability and high fouling tendency are main disadvantages of PES for using in membrane applications which are due to the hydrophobic nature of PES. In recent years some modifications were applied to overcome the disadvantages of based polymers [26].

Cheng et al. [27] built an effective coating layer on the PEG based NF membrane through self-polymerization of mussel-inspired dopamine (DA). The result shows that hydrophilic PEG based membranes after coating with mussel-inspired polydopamine can significantly increase the rejections to salts and other active molecules with only little sacrifice of dual resistance to fouling and chlorine. In another study Cheng et al. [28] synthesized novel polyamide (PA) TFC NF membranes through interfacial polymerization (IP) of amino functional polyethylene glycol (PEG) and trimesoyl chloride (TMC) were designed for achieving dual resistance to fouling and chlorine. Another way to modification of membranes is using additive in the membrane matrix [29-34].

Graphene oxide (GO) sheets have abundant oxygen with functional groups (e.g., hydroxyl, carboxyl, carbonyl, and epoxy groups), resulting in high hydrophilicity for them [29]. By the way, the natural properties of GO nanoplates, such as, good chemical stability, good mechanical properties, high transparency, and large specific surface area, make them as an attractive additive for the preparation of composite membranes [29-34]. Polymeric nanocomposites of graphene derivatives have been used in the preparation of different membranes for fuel cell exchange membrane [35,36], ultrafiltration [33,37,38], nanofiltration [34,39], pervaporation [39] and gas separation [40] applications. Wang et al. improved the water flux of prepared PVDF ultrafiltration membranes by using the GO nanoplates as hydrophilic additive [33].

Shao et al. [41] incorporated GO nanoplates into the PPy/PAN-

†To whom correspondence should be addressed.
E-mail: a.moghadassi@gmail.com, a-moghadassi@araku.ac.ir

H composite SRNF membrane. The result showed that GO incorporation led to a significant enhancement in solvent permeance without compromising RB rejection. Ganesh et al. find that the GO doping into polymer matrix resulted in enhanced hydrophilicity, water flux, and salt rejection property of the polysulfone (PSF) membrane [34].

Furthermore some polymeric materials such as polyaniline can applied with nanoplates as adsorbent [41], which can remove toxic or some other metal ions from water [43-46] due to the existence of nitrogen atom with a lone electron pair as reactive adsorption site. Mansour et al. found that dust which had coated with polyaniline could efficiently adsorb cadmium ions [44]. In another study Belaib et al. coated silica gel and some natural solid materials by polyaniline. They observed copper loading capacity and adsorption kinetics enhanced considerably, using this adsorbent [43]. A polyaniline/inorganic cation-exchanger nanocomposite was fabricated to reach a high capacity ion-exchanger with increased ion exchange rate [46]. A novel mixed matrix pervaporation membrane was successfully prepared by polyvinyl alcohol as base polymer and polyaniline-TiO_2 nanoparticles as modifier [47]. This modified membrane was used for separation of water-isopropanol mixture that resulted in reduction in flux and improvement in selectivity.

In the present work, the influence of blending PANI/GO nanoplates on physico/chemical properties of the polyethersulfone nanofiltration membrane was investigated. PANI/GO was incorporated into the PES matrix. FTIR analysis, SEM, SOM, 3D images surface analysis, water contact angle tests, water content tests, tensile strength tests, porosity tests, salt rejection and flux tests were used in membrane characterization. Na_2SO_4 salt was employed for nanofiltration performance and reusability test.

MATERIALS AND METHODS

1. Materials

Polyethersulfone (PES) provided by Badische Anilin- and Soda-Fabrik (BASF) (Ultrason E6020P, MW=58,000 g/mol), polyvinylpyrrolidone (PVP) provided by Merck (MW=25,000 g/mol), N, N dimethyl acetamide (DMAc, Mw=87.12 g·mol^{-1}) supplied by Merck and deionized water were used as polymer base binder, pore former, solvent and non-solvent, respectively. Graphene oxide nanoplates (2-18 nm with 32 layers) were purchased from US Research Nanomaterials, Inc. (USA). Na_2SO_4 salt was supplied from Merck. Aniline (from Merck, MW=93.13 g·mol^{-1}) and HCl (Mw=36.46 g·mol^{-1} and density=1.19 Kg·Lit^{-1}) manufactured by MOJALLALI chemical laboratories in Iran and ammonium persulfate (Mw=228.2 g·mol^{-1}) from Merck were used for polyaniline preparation. The schematic of chemical structures of graphene oxide is illustrated in Fig. 1.

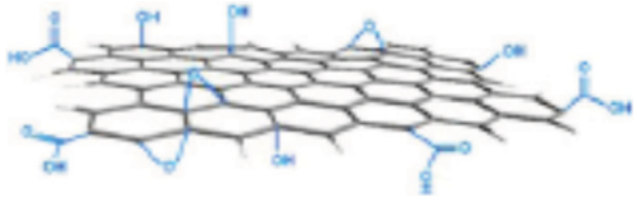

Fig. 1. Schematic of graphene oxide structure.

2. Preparation and Characterization of PANI/GO Nanoplates

The PANI/GO nanoplates were prepared by in situ chemical oxidative polymerization of aniline in the presence of GO nanoplates. According to this method, certain amount of GO nanoplates (mass ratio of GO to aniline monomer was 1 : 2) was added to 50 ml of 0.1 M HCl solution containing 3 ml of distilled aniline monomer and sonicated for 15 min. For good dispersion, the mixture was mechanically stirred. Ammonium persulfate (APS) as reaction initiator, (6 g of APS in 50 ml of 0.1 M HCl solution) was added to the suspension bit by bit to initiate the polymerization of aniline under constant stirring in an ice bath. After 60 min, the polymerization was completed. Dark green color of suspension represents complete polymerization. The product was obtained by filtering the solution. Afterward, it was washed with deionized water and dried in a vacuum oven for 48 hr at 40 °C [42]. For confirmation of PANI formation on the graphene oxide nanoplates, FTIR spectroscopy was applied by Bruker spectrometer (TENSOR 27).

3. Preparation of PANI/GO/PES Mixed Matrix Membrane

Phase inversion induced by immersion precipitation [48,49] was used for nanocomposite membranes preparation. For membrane fabrication, certain amounts of PES (18 wt%) and PVP (1 wt%) were dissolved in solvent (DMAc) by mechanical stirring for 4 hr with stirrer (model: Velp Scientifica Multi 6 stirrer). Afterward, the prepared PANI/GO nanoplates with various concentrations were dispersed into the mentioned polymeric solutions. Dispersing was followed by sonication for 1 hr in an ultrasonic cleaner bath (Parsonic11Smodel, S/N PN-88159, Iran) for breaking up aggregates between nanoplates. The prepared solutions were kept for about 4 h at room temperature without stirring to completely remove the air bubbles, and then they were cast onto clean glass plates with a film applicator with constant thickness of 150 μm. Subsequently, the glass plates were horizontally immersed into distilled water at ambient temperature. After primary phase separation and membrane solidification, the membranes were kept in fresh distilled water for 24 h to ensure the complete solvent extraction. Then, the membranes were placed between two filter paper sheets for 24 h at room temperature for drying. The polymeric solution compositions are shown in Table 1.

4. Characterization of Membranes

4-1. Membrane Morphology

4-1-1. Scanning Electron Microscopy (SEM)

The cross-sectional morphology of membranes was observed

Table 1. Composition of casting solution which used in membrane preparation

Sample no.	Membranes ID	PES (wt%)	PVP (wt%)	DMAc (wt%)	PANI/CO (wt%)
1	M1	18	1	71	0
2	M2	18	1	71	0.05
3	M3	18	1	71	0.1
4	M4	18	1	71	0.5
5	M5	18	1	71	1

PANI/GO weight percentage was based on weight of total solution

using SEM (Seron Technology Inc. Korea) instrument. Before taking SEM images, the membranes were dipped in liquid nitrogen for 5 min and then all the samples were gold sputtered for 10 min and carefully handled to avoid contamination. In this way, the membranes were prepared for SEM images and images were taken at 15 kV in high vacuum conditions.

4-1-2. Scanning Optical Microscopy (SOM)

Scanning optical image analyzing was used for surface characterization of prepared membranes. The instrument used for this aim was Olympus model IX 70, transmission mode with light going through the sample. For taking SOM images the membranes were cut to the appropriate size. Then small pieces of membranes were placed between two glassy blades and the image was taken by the optical microscope.

4-1-3. Surface 3D Images

Surface 3D images were prepared using SOM images and SPIP software (version 6.4.1).

4-2. Water Flux and Salt Rejection

The performance of the prepared membranes was analyzed through a dead-end stirred cell setup (Fig. 1) with effective area of membrane about 11.94 cm^2. The experiment was performed at fixed pressure (5 bar). Permeation flux was calculated by the following equation [50]:

$$Jv=Q/A\cdot t \quad (1)$$

where Jv (L/m^2h), Q (L), A (m^2), t (h) are expressed as permeation flux, content of permeated water, membrane area and permeation time, respectively.

Na_2SO_4 aqueous solution (1,000 mg/L), was used as feed solution for the determining of rejection. Conductivity meter instrument (Ohaus Corporation, S/N B143385306, and U.S.A) was used for measuring the concentration of salt in feed and permeate. The following equation was used for salt rejection calculation [51]:

$$\text{Rejection } \% = 1-\left(\frac{C_p}{C_f}\right)*100 \quad (2)$$

where C_p and C_f are ionic solution concentration in permeate and feed, respectively.

4-3. Mechanical Characterization

Mechanical tensile strength of the fabricated NF membranes was measured by applying ASTM1922-03 standard [52]. For this aim, the membranes were cut into standard shapes and the maximum tolerable load of membranes was measured.

4-4. Water Content

The water content was measured as the weight difference between the dried membranes and wet ones. The wet membranes were weighed initially (OHAUS, Pioneer™, readability: 10-4 g, OHAUS Corp., USA) and then they were dried in an oven (Behdad Co., Model: O5, Iran) at a fixed temperature (50 °C) for 24 hr until constant weight was achieved as dry-membrane. The following equation was used for water content calculation [53]:

$$\%\text{Water content} = \frac{W_w - W_d}{W_w}\times 100 \quad (3)$$

where W_w and W_d are the weight of wet and dried membranes respectively.

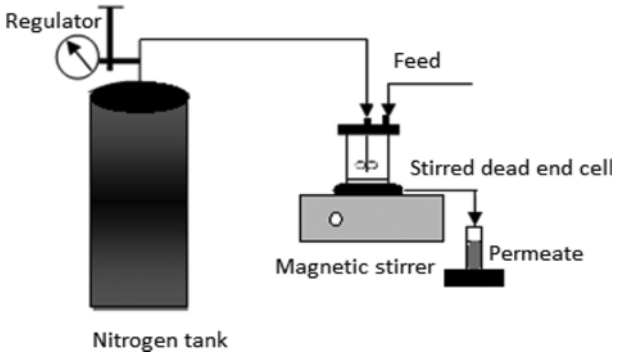

Fig. 2. Schematic diagram of dead end cell experimental set up.

4-5. Water Contact Angle

For observing membrane surface hydrophilicity, the water contact angle was measured by using a contact angle measuring instrument. De-ionized water was the probe liquid in this test. To minimize the experimental errors, the contact angle was measured in three different locations of membranes and the average was reported. All experiments were at ambient temperature.

4-6. Porosity and Pore Size

The following equation can be used for determining the average porosity of membrane (ε) [53]:

$$\varepsilon = \frac{W_{wet} - W_{dry}}{A\times l\times d_w} \quad (4)$$

where A is the membrane effective area (m^2), d_w is the water density (1,000 kg/m^3) and l is the membrane thickness (m).

Additionally, the Guerout-Elford-Ferry equation (Eq. (5)) was used for membranes' mean pore radius (r_m) calculation. This equation is on basis pure water flux [54,55].

$$r_m = \sqrt{\frac{(2.9-1.75\varepsilon)8\eta l Q}{\varepsilon\times A\times \Delta P}} \quad (5)$$

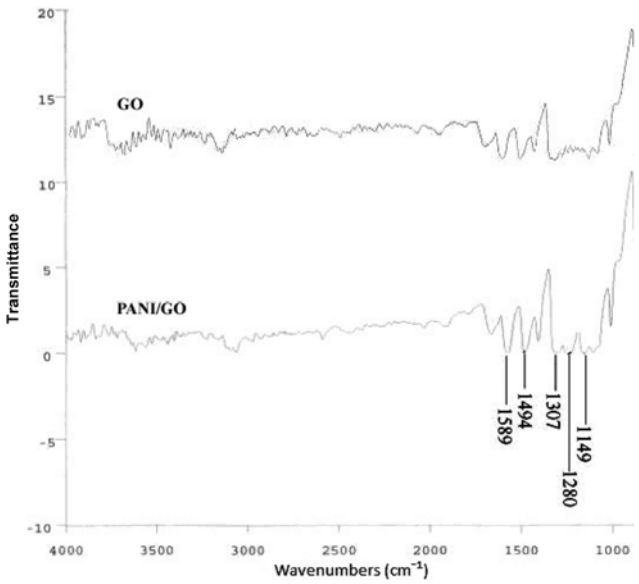

Fig. 3. FTIR spectra of GO and PANI/GO nanoplates.

where η is the water viscosity (8.9×10^{-4} Pa·s), Q is the volume of permeated pure water per unit time (m^3/s), and ΔP is the operational pressure (0.5 MPa).

4-7. Antifouling Ability of the Membranes

The antifouling properties of the prepared membranes were measured by flux decreased ratio measuring through the continuously filtration experiment. The flux decreased ratio was calculated according to Eq. (6) [56]:

$$M\% = \frac{J_0 - J_1}{J_0} * 100\% \quad (6)$$

where J_0 is the original flux, J_1 is the flux after continuously filtrating for 90 min.

RESULT AND DISCUSSION

1. FTIR Analysis

With respect to FTIR spectra of graphene oxide and PANI/GO depicted in Fig. 3, the PANI/GO nanoplates showed sharper peaks at 1307 (QBB, QBQ), 1494 (N-B-N) and 1589 (N-Q-N) compared to graphene oxide, which can confirm the presence of PANI on the GO nanoplates, and also peaks at 1149, 1280 (C-N) cm verify

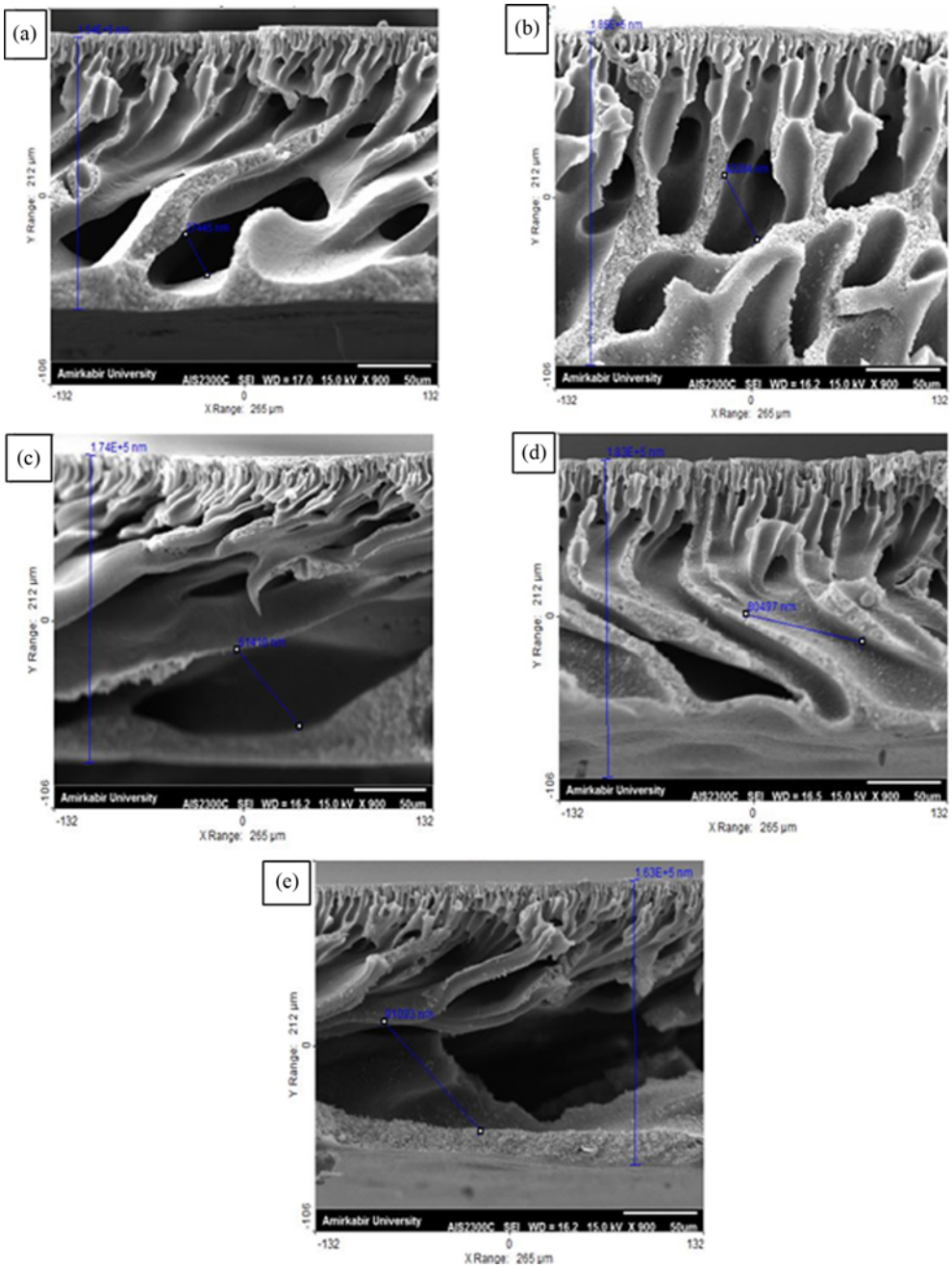

Fig. 4. The SEM images of cross-sectional of fabricated membranes with different concentrations of PANI/GO nanocomposite plates: (a) Sample 1, (b) sample 2, (c) sample 3, (d) sample 4 and (f) sample 5.

formation of PANI on graphene oxide nanoplates [42].

2. Membrane Morphology

The SEM cross sectional images of prepared NF membrane with different concentration of PANI/GO as modifier are shown in Fig. 4. According to the results, all samples have an asymmetric structure with a dense top layer and a porous sub-layer. As can be seen, the increase of PANI/GO concentration in to the casting solution caused an increase of the membrane porosity and size of sub-layer's channels. This can be attributed to phase inversion time of casting film in coagulation bath during membrane preparation. PANI/GO is a hydrophilic additive [42], so adding it to the casting solution can result in a lower phase inversion time, which leads to instantaneous demixing [57]. Increase of PANI/GO content as a hydrophilic additive can increase the diffusion rate of non-solvent into the casting film, resulting in accelerating the precipitation rate of PES in non-solvent and so incrementing the porosity [58].

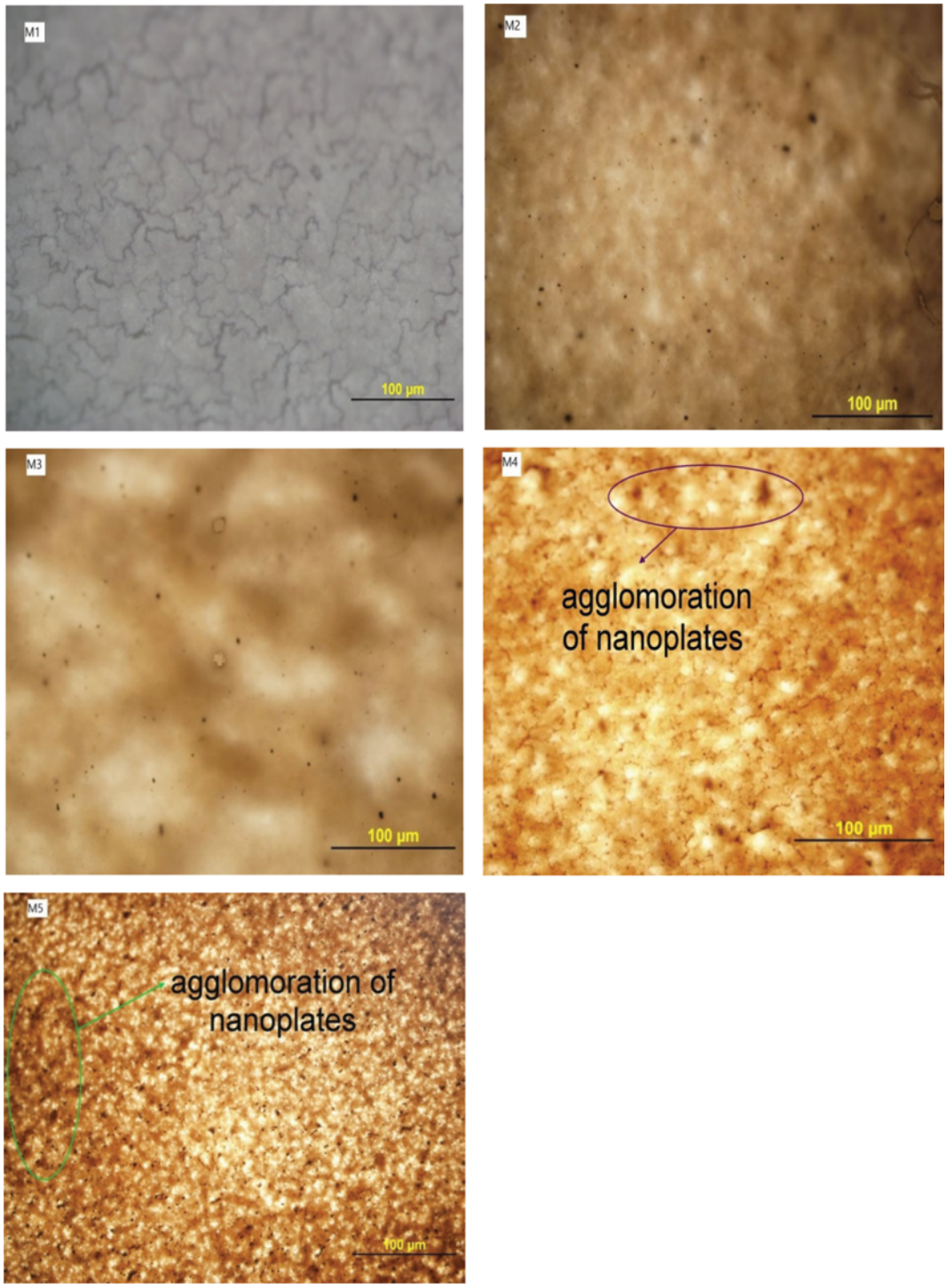

Fig. 5. SOM images of prepared membranes.

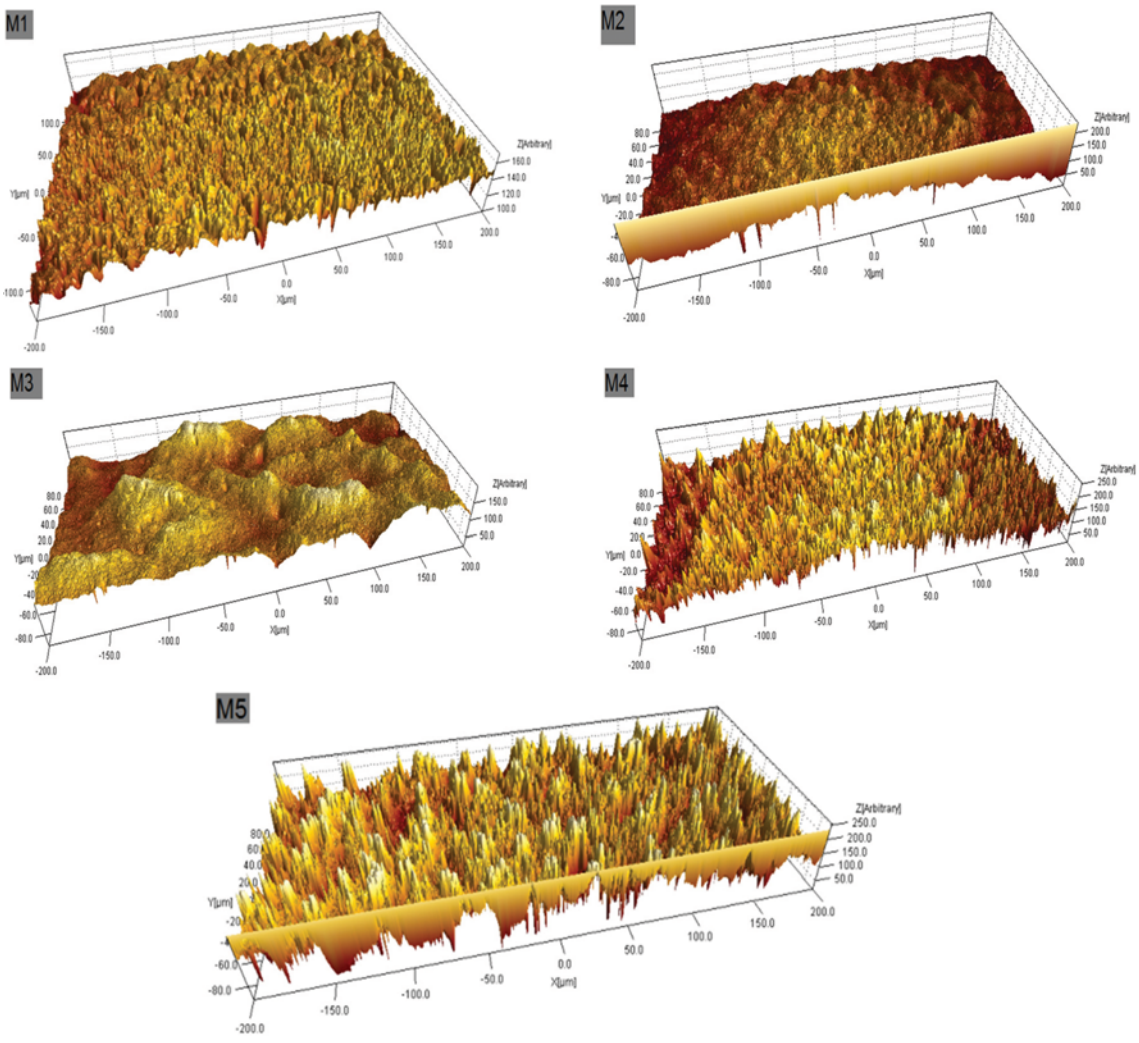

Fig. 6. Surface roughness images.

To investigate PANI/GO distribution in the membrane matrix/surface, SOM images were carried out. As shown in Fig. 5, PANI/GO distributed uniformly in M2 and M3 at the surface of the membranes. But M4 and M5 showed agglomeration in specified zones. Agglomeration in M4 and M5 probably refers back to the high concentration of nanoplates.

Roughness images are shown in Fig. 6. According to this figure, M1 introduced a rough surface. M2 and M3 show reduction of rough in their surface, which may be related to uniform particles distribution in the surface of pores, leading to smoother surface compared to M1. As can be seen, the membrane roughness at the surface was increased again for M4 and M5. As can be seen in Fig. 7, in the membranes with high concentration of PANI/GO, most of nanoplates moved to the surface of the membrane during phase inversion process, so aggregation of nanoplates on the top surface in M4 and M5 could be the main reason for roughness increment.

3. Effect of PANI/GO Concentration on Membrane Permeability and Salt Rejection

Permeability and salt rejection are two important determinants of membrane performance. Membrane salt rejection was tested

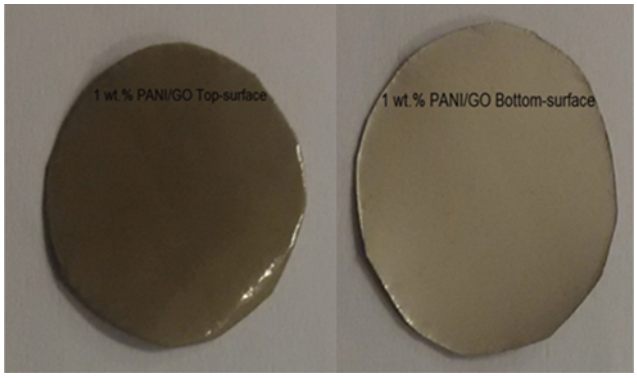

Fig. 7. Top and bottom surface of membrane with 1 wt% PANI/GO dosage.

with Na_2SO_4 aqueous solution. The effect of PANI/GO concentration on permeability flux and salt rejection is shown in Fig. 8. The results revealed that salt rejection increases with increase of PANI/GO concentration into the casting solution, except in M5. As men-

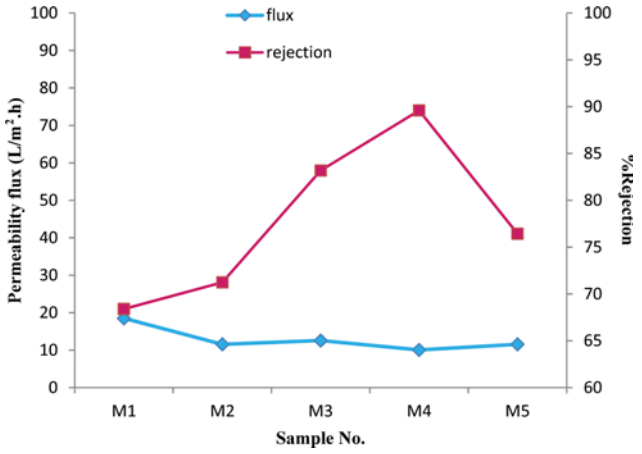

Fig. 8. The effect of PANI/GO nanocomposite plate's concentration on membrane performance.

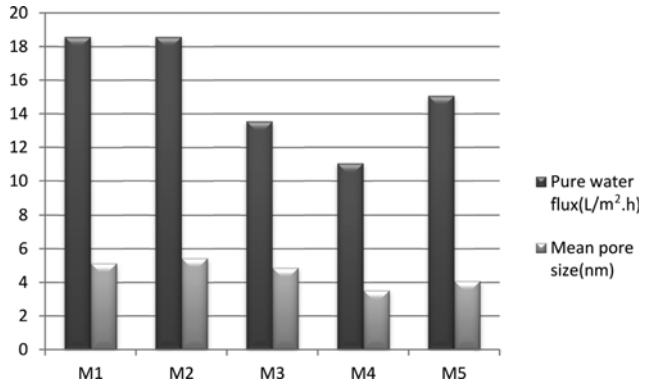

Fig. 10. The effect of PANI/GO nanocomposite plate's concentration on pure water flux and mean pore size.

tioned earlier, polyaniline has adsorption characteristic [43]. This property can improve surface/depth filtration mechanism during filtration experiment. So, the adsorption characteristic of PANI/GO can be a reason for rejection improvement by increasing of PANI/GO concentration. Moreover, because of hydrophilic nature of graphene oxide [59], lower precipitation of solute particles solved into the water on to the membrane surface can result in a higher rejection rate. This can be another reason for rejection improvement by use of PANI/GO into the membrane matrix. Rejection decreasing in M5 partly can be related to PANI/GO agglomeration in high loading range (see Fig. 9), which restricts effective adsorption sites of the nanoplates, leading to reduction of the membrane surface functional groups, too. Additionally, another part of rejection reduction in M5 can be due to increase of the membrane mean pore size compared to M4 (see Fig. 10).

Additionally, the results of permeability flux shown in Fig. 8, indicated that a decline in permeability flux was observed by increasing of PANI/GO concentration. As seen in Fig. 8, unfilled PES membrane has the most high permeability flux compared to others. Addition of PANI/GO into the casting solution leads to the reduction of permeability flux. This phenomenon can be related to the pore blockage/filling (see Fig. 9) that occurred with PANI/GO particles which were moved to the membranes' top surface during phase inversion process because of high hydrophilicity of PANI/GO. In this situation the presence of PANI/GO in the top surface reduces pathways size/number, leading to lower areas for passing water through the membrane, which results on the lower flux. Fig. 7 shows graphical images of top/bottom surface of prepared mixed matrix membrane filled with 1 wt% of nanoplates. The results revealed that hydrophilic composite PANI/GO nanoplates moved to the top surface during phase inversion process. As can be seen in Fig. 4 (SEM images), pristine PES membrane has minimum thickness compared to others. The membrane thickness measured in Fig. 4 indicated higher thickness for membranes filled with PANI/GO. This can be another reason for decrease of permeability flux for membrane filled with PANI/GO.

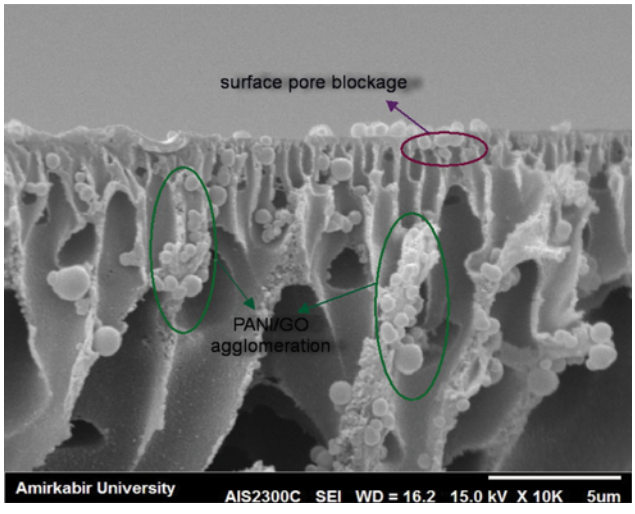

Fig. 9. Surface pore blockage and nanocomposite plates agglomeration in 1 wt% PANI/GO nanocomposite plates.

4. Membrane Water Content

The membrane water content is a criterion of hydrophilicity and swelling [60-62]. Table 2 shows the effect of PANI/GO concentration on the membrane water content. According to Table 2, filled membranes with PANI/GO have more water content than bare PES (M1). This may be partly due to the hydrophilic characteristic of PANI/GO nanoparticles and partly to the increase of sublayer pore size and porosity (see Fig. 4 and Table 2) [63]. The results indicated that the maximum value of water content belonged to M2 and it was decreased by addition of higher PANI/GO concen-

Table 2. Water content, porosity and water contact angle of fabricated membranes

Membrane ID	Water content %	Porosity %	Water contact angle (°)
M1	73.08	65	65.38
M2	81.76	67	46.97
M3	75.68	70	40.14
M4	75.59	71	37
M5	74.08	71.5	42

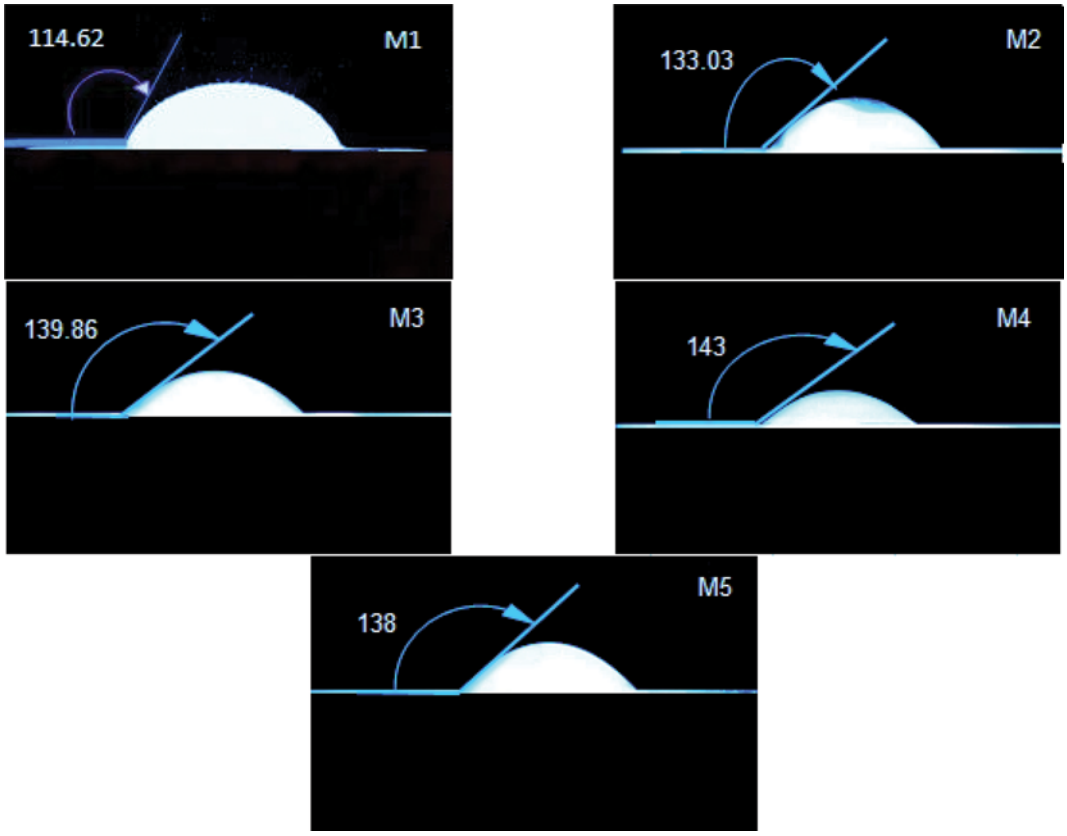

Fig. 11. Position of water drops on surface of the membranes.

trations (M3, M4 and M5) compared to M2. The reduction of water content at M3, M4 and M5 may be due to surface pore blocking by the additive particles leading to the lower water entrance to the membranes and lower water storage in the membranes [64].

5. Effect of PANI/GO Concentration on Water Contact Angle

Water contact angle determining can show hydrophilicity of surface membrane. Fig. 11 illustrates the position of water droplets on the top surface of the prepared membranes. Lower contact angle represents more hydrophilicity of membrane surface. As shown in Table 2, contact angle decreased with addition PANI/GO nanoplates into the polymer matrix. Bare PES membrane showed the highest water contact angle about 65.38. Addition of nanoplates reduced the water contact angle form 65.38 for bare PES membrane to 37 for membrane filled with 0.5 wt% PANI/GO. However, the membrane filled with 1 wt% of PANI/GO had larger contact angle compared to other modified membranes. This can be partly related to agglomeration and decreased effective surfaces of the nanoplates in the high blending ratio, resulting in decline of the membrane surface functional groups (see Fig. 6 and section 3.3) [59], and partly due to the higher surface roughness of M5 compared others (see Fig. 6). According to Fig. 6, the convex parts of M5 are sharp, resulting in less hydrophilicity compared to others [58].

6. Surface Mean Pore Radius and Pure Water Flux

The results of mean pore radius calculated with Eq. (5) are shown in Fig. 10. The results indicated that mean pore radius of the membranes decreased with increase of PANI/GO concentration up to 0.5 wt% and again increased with higher additive loading range,

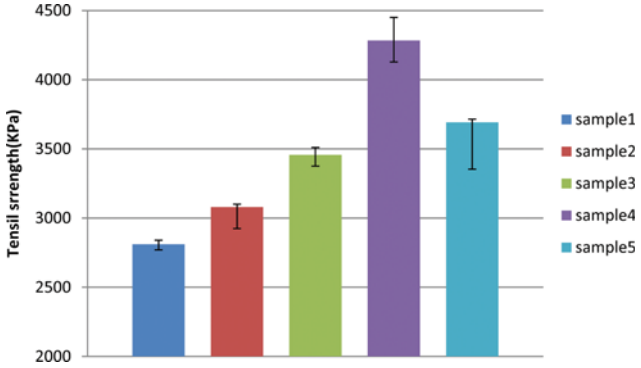

Fig. 12. The effect of PANI/GO nanocomposite plate's concentration on tensile strength.

which is in very good agreement with pure water flux trend plotted in Fig. 10. Increase of pure water flux in M5 can be attributed to lower thickness of this sample compared to other modified membranes (see SEM images).

7. Membrane Mechanical Tensile Strength

The tear resistance as a mechanical property of the prepared membranes was tested according to ASTM1922-03. Obtained results (Fig. 12) showed that mechanical strength of modified membrane was increased obviously by using PANI/GO into the casting solution compared to unmodified membrane (bare PES one). The results revealed that PANI/GO nanoplates can act as a physical cross-linking agent in membrane structure to link the polymer chain and

to increase its rigidity [65,66]. Thus, membranes with higher concentration of PANI/GO nanoplates could tolerate higher load stress of the load. Decrease of mechanical tensile strength in M5 compared to M4 may be related to aggregation of additive particles in high loading range of nanoplates (Fig. 9) [67]. This reduction can be also due to the high porosity and increase of channels' size of M5 (Fig. 4), which leads to a loose structure for the membrane and decreases the membranes' tensile strength.

8. Analysis of the Antifouling Ability of the Membranes

The decreased flux ratio of membranes can be used to determine the antifouling performance of prepared membranes [68]. Fig. 13 illustrates the permeate fluxes of the fabricated membranes, when Na_2SO_4 is tested solution. As can be seen, at the first of filtration, flux was decreased in all the membranes; after that it reached a relatively stable plateau over time. All the modified membranes have lower flux decrease compared to bare PES. The data in Table 3 are calculated from Fig. 13. Lower decrease flux ratio implies better antifouling performance. According to Table 3, modification of membranes improved antifouling ability of membranes. The membrane with 0.5 wt% PANI/GO shows the highest antifouling ability.

The flux decreased ratio of M4 membrane is only 5% after 90 min of filtering, whereas the flux decreased ratio of the unfilled PES membrane is 66.67%.

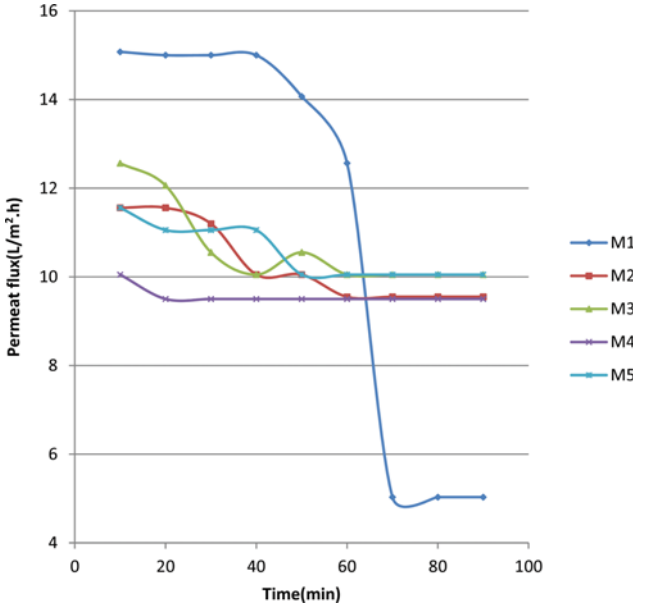

Fig. 13. Permeate flux (5 bar) decline with time for the different membranes measured by Na_2SO_4 aqueous solution.

Table 3. Data of decreased flux ratio after 90 min of filtrating for each membrane

Membrane ID	Decreased flux ratio (%)
M1	66.67
M2	17.39
M3	20
M4	5
M5	13.04

CONCLUSION

Phase-inversion method was used for fabrication of a set of membranes. The effects of PES modification by PANI/GO nanoplates on properties of the membranes were carried out. The main conclusions are as follows:

1. All the modified membranes had lower water contact angle compared to unfilled PES. Water contact angle of bare PES was 65.38°, while this amount was 37° for membrane with 0.5 wt% of PANI/GO. This means modification increased the membranes' hydrophilicity.

2. The porosity of membranes increased by adding PANI/GO nanoplates.

3. Addition of PANI/GO nanoplates significantly improved the salt rejection of the prepared membranes from 68.4% fore unmodified PES to 89.6% for M4.

4. Incorporation of PANI/GO nanoplates into the PES based mixed matrix membrane significantly increased the mechanical strength of the membranes. Mechanical strength of the membrane with 0.5 wt% PANI/GO concentration was nearly 50% more than pristine PES.

5. Addition of PANI/GO improved the antifouling performance of the prepared membranes. 0.5 wt% dosage of PANI/GO membrane had only 5% permeate flux decline ratio after 90 min of Na_2SO_4 solution filtration, while it was 66.67% for the virgin PES.

Regarding the obtained hydrophilicity, salt rejection, mechanical properties and antifouling ability, 0.5 wt% of PANI/GO was found as the optimum concentration for PANI/GO in the casting solution. This study showed that polyaniline/graphene oxide nanocomposite plate is a suitable modifier in the membrane fabrication from the perspective of hydrophilicity, mechanical properties, salt rejection performance and antifouling ability improvement.

ACKNOWLEDGEMENT

The authors gratefully acknowledge Arak University for the financial support during this research.

REFERENCES

1. V. V. Goncharuk, A. A. Kavitskaya and M. D. Skil'skaya, *J. Water Chem. Technol.*, **33**, 37 (2011).
2. A. Rahimpour, B. Rajaeian, A. Hosienzadeh, S. S. Madaeni and F. Ghoreishi, *Desalination*, **265**, 190 (2011).
3. J. Luo, L. Ding, X. Chen and Y. Wan, *Sep. Purif. Technol.*, **66**, 429 (2009).
4. M. R. Sohrabi, S. S. Madaeni, M. Khosravi and A. M. Ghaedi, *Sep. Purif. Technol.*, **75**, 121 (2010).
5. N. Capelle, P. Moulin, F. Charbit and R. Gallo, *J. Membr. Sci.*, **196**, 125 (2002).
6. M. J. Gonzalez-Munoz, M. A. Rodriguez, S. Luque and J. R. Alvarez, *Desalination*, **200**, 742 (2006).
7. R. J. Petersen, *J. Membr. Sci.*, **83**, 81 (1993).
8. A. Z. Muhammad, A. W. Mohammad and H. Nidal, *Desalination*, **192**, 262 (2006).
9. C. C. Yang, Y. J. James Li and T. H. Liou, *Desalination*, **276**, 366

(2011).
10. N. Maximous, G. Nakhla and W. Wong, *J. Membr. Sci.*, **341**, 67 (2009).
11. Y. N. Yang and P. Wang, *Polymer*, **47**, 2683 (2006).
12. N. A. A. Sani, W. J. Lau and A. F. Ismail, *Korean J. Chem. Eng.*, **32**, 743 (2015).
13. N. Ghaemi, S. S. Madaeni, A. Alizadeh, P. Daraei, M. M. S. Badieh, M. Falsafi and V. Vatanpour, *Sep. Purif. Technol.*, **96**, 214 (2012).
14. N. Ghaemi, S. S. Madaeni, A. Alizadeh, P. Daraei, V. Vatanpour and M. Falsafi, *Desalination*, **290**, 99 (2012).
15. C. Zhao, J. Xue, F. Ran and S. Sun, *Prog. Mater. Sci.*, **58**, 76 (2013).
16. A. L. Ahmad, A. A. Abdulkarim, B. S. Ooi and S. Ismail, *Chem. Eng. J.*, **223**, 246 (2013).
17. J. H. Choi, K. Fukushi and K. Yamamoto, *Sep. Purif. Technol.*, **52**, 470 (2007).
18. J. C. Jansen, S. Darvishmanesh, F. Tasselli, F. Bazzarelli, P. Bernardo, E. Tocci, K. Friess, A. Randova, E. Drioli and B. Van der Bruggen, *J. Membr. Sci.*, **447**, 107 (2013).
19. G. d. Kang and Y. M. Cao, *J. Membr. Sci.*, **463**, 145 (2014).
20. C. V. Gherasim, J. Cuhorka and P. Mikulášek, *J. Membr. Sci.*, **436**, 132 (2013).
21. M. Namvar-Mahboub and M. Pakizeh, *Sep. Purif. Technol.*, **119**, 35 (2013).
22. S. S. Shenvi, S. A. Rashid, A. F. Ismail, M. A. Kassim and A. M. Isloor, *Desalination*, **315**, 135 (2013).
23. N. Rakhshan and M. Pakizeh, *Korean J. Chem. Eng.*, **32**, 2524 (2015).
24. M. Namvar-Mahboub and M. Pakizeh, *Korean J. Chem. Eng.*, **31**, 327 (2013).
25. A. Rahimpour, *Korean J. Chem. Eng.*, **28**, 261 (2010).
26. Y. Mansourpanah, S. S. Madaeni, A. Rahimpour, M. Adeli, M. Y. Hashemi and M. R. Moradian, *Desalination*, **277**, 171 (2011).
27. Q. C. Xi, Z. Cong, X. W. Zhen and S. Lu, *J. Membr. Sci.*, **499**, 326 (2016).
28. Q. C. Xi, L. Yuyan, G. Zhanhu and S. Lu, *J. Membr. Sci.*, **493**, 156 (2015).
29. G. Gonalves, P. A. A. P. Marques, A. Barros-Timmons, I. Bdkin, M. K. Singh, N. Emami and J. Gracio, *J. Mater. Chem.*, **20**, 9927 (2010).
30. R. Van Noorden, *Nature*, **442**, 228 (2006).
31. X. Zhang, B. Wang, J. Sunarso, S. Liu and L. Zhi, *WIREs EnergyEnviron.*, **1**, 317 (2012).
32. M. El Achaby, F. Z. Arrakhiz, S. Vaudreuil, E. M. Essassi and A. Qaiss, *Appl. Surf. Sci.*, **258**, 7668 (2012).
33. Z. Wang, H. Yu, J. Xia, F. Zhang, F. Li, Y. Xia and Y. Li, *Desalination*, **299**, 50 (2012).
34. B. M. Ganesh, A. M. Isloor and A. F. Ismail, *Desalination*, **313**, 199 (2013).
35. A. Enotiadis, K. Angjeli, N. Baldino, I. Nicotera and D. Gournis, *Small*, **8**, 3338 (2012).
36. Y. Heo, H. Im and J. Kim, *J. Membr. Sci.*, **425**, 11 (2013).
37. Y. Zhao, Z. Xu, M. Shan, C. Min, B. Zhou, Y. Li, B. Li, L. Liu and X. Qian, *Sep. Purif. Technol.*, **103**, 78 (2013).
38. J. Zhang, Z. Xu, W. Mai, C. Min, B. Zhou, M. Shan, Y. Li, C. Yang, Z. Wang and X. Qian, *J. Mater. Chem.*, **1**, 3101 (2013).
39. N. Wang, S. Ji, G. Zhang, J. Li and L. Wang, *Chem. Eng. J.*, **213**, 318 (2012).
40. J. Liang, Y. Huang, L. Zhang, Y. Wang, Y. Ma, T. Guo and Y. Chen, *Adv. Funct. Mater.*, **19**, 2297 (2009).
41. S. Lu, C. Xiquan, W. Zhenxing, M. Jun and G. Zhanhu, *J. Membr. Sci.*, **452**, 82 (2014).
42. P. Daraei, S. S. Madaeni, N. Ghaemi, E. Salehi, M. Khadivi, R. Moradian and B. Astinchap, *J. Membr. Sci.*, **415**, 250 (2012).
43. F. Belaib, A. H. Meniai, M. Bencheikh-Lehocine, A. Mansri, M. Morcellet, M. Bacquet and B. Martel, *Desalination*, **166**, 371 (2004).
44. M. S. Mansour, M. E. Ossman and H. A. Farag, *Desalination*, **272**, 301 (2011).
45. A. A. Khan and L. Paquiza, *Desalination*, **265**, 242 (2011).
46. L. Ai and J. Jiang, *Mater. Lett.*, **65**, 1215 (2011).
47. S. A. Patil and T. M. Aminabhavi, *J. Membr. Sci.*, **281**, 95 (2006).
48. K. Kimmerle and H. Strathmann, *Desalination*, **79**, 283 (1990).
49. J. G. Wijmans, J. P. B. Baaij and C. A. Smolders, *J. Membr. Sci.*, **14**, 263 (1983).
50. R. Han, S. Zhang, C. Liu, Y. Wang and X. Jian, *J. Membr. Sci.*, **345**, 5 (2009).
51. H. S. Lee, S. J. Im, J. H. Kim, H. J. Kim, J. P. Kim and B. R. Min, *Desalination*, **219**, 48 (2008).
52. A. Gholami, A. R. Moghadassi, S. M. Hosseini, S. Shabani and F. Gholami, *J. Ind. Eng. Chem.*, **20**, 1517 (2014).
53. M. Sivakumar, A. K. Mohanasundaram, D. Mohan, K. Balu and R. Rangarajan, *J. Appl. Polym. Sci.*, **67**, 1939 (1998).
54. V. Vatanpour, S. S. Madaeni, R. Moradian, S. Zinadini and B. Astinchap, *Sep. Purif. Technol.*, **90**, 69 (2012).
55. N. A. A. Hamid, A. F. Ismail, T. Matsuura, A. W. Zularisam, W. J. Lau, E. Yuli Wati and M. S. Abdullah, *Desalination*, **273**, 85 (2011).
56. L. Shen, X. Bian, X. Lu, L. Shi, Z. Liu, L. Chen, Z. Hou and K. Fan, *Desalination*, **293**, 21 (2012).
57. E. Bagheripour, A. R. Moghadassi and S. M. Hosseini, *Asia-Pac. J. Chem. Eng.*, **10**(5), 791 (2015).
58. X. Chang, Z. Wang, S. Quan, Y. Xu, Z. Jiang and L. Shao, *Appl. Surf. Sci.*, **316**, 537 (2014).
59. S. Zinadini, A. A. Zinatizadeh, M. Rahimi, V. Vatanpour and H. Zangeneh, *J. Membr. Sci.*, **453**, 292 (2014).
60. E. Bagheripour, A. R. Moghadassi and S. M. Hosseini, *Korean J. Chem. Eng.*, **33**(4), 1462 (2016).
61. M. Sivakumar, D. Raju Mohan and R. Rangarajan, *J. Membr. Sci.*, **268**, 208 (2006).
62. S. Pourjafar, A. Rahimpour and M. Jahanshahi, *J. Ind. Eng. Chem.*, **18**, 1398 (2012).
63. P. Mobarakabad, A. R. Moghadassi and S. M. Hosseini, *Desalination*, **365**, 227 (2015).
64. S. M. Hosseini, A. R. Hamidi, S. S. Madaeni and A. R. Moghadassi, *Korean J. Chem. Eng.*, **32**(3), 429 (2015).
65. M. Mulder, Basic Principles of Membrane Technology, 2nd Ed. Kluwer (1996).
66. J. F. Li, Z. L. Xu, H. Yang, L. Y. Yu and M. Liu, *Appl. Surf. Sci.*, **255**, 4725 (2009).
67. Y. Liu, J. Wang, H. Zhang, C. Ma, J. Liu, S. Cao and X. Zhang, *J. Power Sources*, **269**, 898 (2014).
68. C. J. Liao, J. Q. Zhao, P. Yu, H. Tong and Y. B. Luo, *Desalination*, **260**, 147 (2010).